

## REDUCED STIFFNESS AXIAL LOAD BUCKLING OF CYLINDERS

J. G. A. CROLL and C. P. ELLINAS  
 University College London, Gower Street, London WC1E 6BT, England

(Received 15 April 1982)

**Abstract**—A reduced stiffness method is presented for the estimation of lower bounds to the imperfection sensitive general buckling of axially loaded, orthotropically stiffened, elastic cylinders. It predicts many previously inexplicable empirical observations and provides lower bounds to the scatter of available test buckling loads, thus becoming useful as a design tool.

### NOTATION

$d_r$	ring stiffener depth
$d_s$	stringer stiffener depth
$E$	modulus of elasticity
$E_x^F, E_\theta^F$	fundamental state membrane strains
$i$	number of circumferential waves
$j$	number of axial half waves
$k$	flexural restraint coefficient
$K$	extensional stiffness
$l$	length of cylinder
$m_x, m_{x\theta}, m_\theta$	incremental moment resultants
$n_r$	number of ring stiffeners
$n_s$	number of stringer stiffeners
$n_x, n_{x\theta}, n_\theta$	incremental stress resultants
$N_x^F, N_\theta^F$	fundamental state stress resultants
$r$	radius of cylinder
$s_r$	ring stiffener spacing, $\equiv l/(n_r + 1)$
$s_s$	stringer stiffener spacing, $\equiv 2\pi r/n_s$
$t$	thickness of cylinder skin
$t_r$	thickness of ring stiffener
$t_s$	thickness of stringer stiffener
$u, v, w$	incremental displacements in $x, \theta$ and normal directions
$U_B, U_M$	bending and membrane strain energy contributions
$V$	incremental total potential energy
$\bar{V}_M^x, \bar{V}_M^\theta, \bar{V}_M^0$	axial and circumferential components of non-linear membrane energy
$x$	axial spatial coordinate
$\alpha_x, \alpha_\theta$	orthotropic axial and circumferential extensional stiffness ratios
$\epsilon_x, \epsilon_{x\theta}, \epsilon_\theta$	incremental membrane strains
$\eta$	efficiency parameter
$\theta$	circumferential spatial coordinate
$\lambda$	non-dimensional axial wavelength parameter, $\equiv j\pi r/l$
$\mu$	Poisson's ratio
$\xi_y$	modal reduction factor, $\equiv \sigma_c^*/\sigma_c$
$\rho$	knock-down factor, $\equiv \sigma_{cm}^*/\sigma_{cm}$
$\sigma$	axial stress
$\sigma_c, \sigma_c^*$	classical and reduced stiffness critical stress
$\sigma_{cm}, \sigma_{cm}^*$	classical and reduced stiffness minimum critical stress
$\chi_x, \chi_{x\theta}, \chi_\theta$	incremental bending strains

#### *Subscripts*

$B$	bending energy component
$c$	belonging to critical mode
$cm$	belonging to minimum critical mode
$exp$	experimental
$ij$	belonging to mode $(i, j)$
$r$	ring stiffener parameter
$s$	stringer stiffener parameter
$th$	theoretical
$x$	belonging in axial direction
$\theta$	belonging in circumferential direction

*Superscripts*

$F$	belonging to fundamental state
$x$	belonging to axial direction
$\theta$	belonging to circumferential direction
'	stresses and strains linearly dependent on displacements
"	stresses and strains quadratically dependent on displacements
*	corresponding to reduced stiffness model
$\sim$	containing non-linear strains
$\approx$	containing non-linear stresses
-	evaluated at the centroid of the orthotropic cross-section

## INTRODUCTION

The increased scope and ease of analysis offered by the still emerging and radically changing computation environment has demonstrably broadened the range of structural systems for which theoretical analysis can now be contemplated. But with the associated changes in the nature of analysis many engineers are concerned that much of importance to the creative design process is in danger of being lost. Traditional analysis procedures for all their tedium, or perhaps even because of it, meant that the design analyst accumulated a wealth of physical and even intuitive understanding of the relationships between changes in the forms of structures and their response. In contrast, modern, usually computer based, analysis has a tendency towards abstraction from both its physical base and its design context, relying heavily on elegant but physically remote analytical and computational methods, that no longer provide a direct vehicle for understanding the physics of structural behaviour.

This general tendency towards increasing of analysis and separation between computation and analysis on one hand, and physics and design on the other can be clearly discerned in the ways in which non-linear buckling phenomena are so often translated into design. For what is perhaps the most notorious of shell buckling problems, the axially loaded cylinder, the present paper illustrates how the direct incorporation of physical ideas on non-linear post buckling behaviour can provide a reliable and simple analysis that is ideally suited to design. It will be shown how by incorporating these conceptually simple ideas into a reduced stiffness model for the general elastic buckling analysis of axially loaded orthotropically stiffened cylinders, it is possible to predict a number of important but previously inexplicable aspects of their empirical behaviour. Apart from predicting the unique modes observed to trigger buckling the reduced stiffness eigenvalue analysis of buckling is shown to provide reliable lower bounds to the scatter of test buckling loads. While many of these aspects have been described in recent publications[1-3], the present paper develops the analytic simplicity of the method to provide compact theoretical lower bounds to test buckling loads. These, it is argued, are ideally suited to design and may be effectively employed at the early stages of conceptual design where major improvements in structural efficiency can be achieved.

Although concentrating on the elastic buckling of axially loaded cylinders the general philosophy of analysis described is suggested to have very much wider potentialities. For the imperfection sensitive buckling of other shell forms and other loading cases, and for the interaction between elastic and plastic non-linearities the method has already been shown to provide interesting practical possibilities[4].

## A LOWER BOUND BUCKLING CONCEPT

Before discussing the specific characteristics of axially loaded cylinder buckling it will be helpful to recall one or two general properties of systems exhibiting significant non-linearities in their post-buckling behaviour, and identify the circumstances in which their buckling behaviour is likely to be sensitive to the forms and magnitudes of the small initial imperfections. The *first* observation that can be made is that practically *significant non-linearity in the post-buckling response can only occur where* the physical conditions of the problem enable *changes in the membrane stiffness* (of equivalently energy) from that associated with the critical loads. This feature is of course well recognised by the fact that it is membrane non-linearities that are usually incorporated into our non-linear analyses. The very slight non-linearities in bending stiffness occurring in advanced post-critical states are usually assumed to involve deformations whose magnitudes are so large as to be outside any practical range.

Whether these changes in membrane stiffness lead to increases or decreases in the structure's resistance to buckling deformations, that is whether the buckling is stabilising or destabilising, depends upon the extent to which the membrane energy actually provides a stabilising contribution to the initial resistance to buckling deformations. In shells it is often the importance of this membrane energy in the critical modes that gives them their advantage so far as buckling is concerned. But equally it is the presence of this membrane stiffness in the critical modes that creates so many of the problems in understanding shell buckling behaviour. There are many instances where the combination of initial imperfection and the coupling between the various possible buckling modes can lead to an erosion of this vital membrane stiffness in the buckling response. Where this occurs, and it is to a large extent governed by the physical characteristics of a particular problem, the reduction in membrane stiffness with increasing buckling deformation is associated with a loss of post-buckled load carrying capacity. This leads to the *second* general observation that the *non-linearity in post-buckling response can only be unstable where the membrane stiffness, or again related energy, contributes to the structure's resistance to deformation in the associated critical mode*. Put more simply, a change in post-buckling membrane stiffness *can* only lead to a loss of stiffness if there is already positive membrane resistance, or energy, in the critical mode. As to whether or not the response *will* be unstable depends upon the prevailing physical conditions and the success of the lower bound methods depends upon the ability to define which of the membrane stiffness components in the critical mode will be eroded in the post-critical response.

By identifying those components of the membrane stiffness, or equivalently energy, that may be eroded during buckling, the reduced stiffness method then consists of an eigenvalue analysis for the same system but with the appropriate components of membrane energy eliminated. For the interactive buckling of built-up columns and plates the related reduced modulus procedure is well established [5-8]. In some shells it would appear that all the initial membrane strain energy may be lost, and applications of this approach may be found in Ref. [9]. In other situations, such as the present classes of axially loaded cylinder, only parts of the initial membrane energy would appear to be lost at the instant of imperfection generated snap buckling. As an illustration of how the reduced stiffness concept can lead to practically useful results, the following section reiterates some of the features of the buckling of axially loaded cylinders central to the reduced stiffness method.

## ANALYSIS OF AXIALLY LOADED CYLINDER BUCKLING

### *Background*

Recent regeneration of interest in the buckling of stiffened cylinders derives from the rapidly evolving applications of these structural components in marine structures. With exploration and development taking place in oceans of increasing depth and environmental hostility, and with the proliferation of different classes of platform in which the shell components are being called upon to provide different combinations of bouyancy and vertical load capacity, a number of important and as yet imperfectly understood buckling problems are emerging. Under arbitrary combinations of axial and radial pressure loads and making due allowance for the interactions between elastic and plastic behaviour, what are the safe loads that may be sustained by these shells, what choices of stringer and ring stiffening should be made to improve the structural and functional efficiency, under what circumstances is it possible for the various possible buckling modes to interact and how can this be allowed for or avoided in design, and how are all these aspects affected by the precise nature of end supports and initial imperfection forms relating to these components? In conceiving of the possibility that non-linear computer based solution codes will provide such comprehensive information and understanding, it is salutary to remind ourselves of the current status of theoretical developments in cylindrical shell buckling.

Despite four decades of at times frantic activity in the non-linear analysis of axial load buckling of isotropic cylinders, it is probably still true to say that their observed behaviour is only partially understood. These developments have seen a growth in the sophistication of the non-linear buckling codes attempting to account for the observed imperfection

sensitivity and forms of buckling. For an extensive list of references see[10]. They have also been accompanied by an increase in the precision with which the test programmes themselves are carried-out. For very small imperfections, in which the radial geometric errors are orders of magnitude less than the thickness, the gap between theory and test has undoubtedly been narrowed. The careful control of axisymmetric imperfections in Tennyson's tests[11], for example, has provided a close quantitative confirmation of the asymptotic predictions of Koiter's special theory[12]. And the prediction of a succession of post-buckling configurations provided by inter alia Yamaki[13] and Esslinger and Geier[14] show similarities to observed post-buckling behaviour. But for moderate to large imperfections of the same order as the thickness of the shell, considerable discrepancies between theoretical predictions and experimental observation remain. For marine structures whose scale and in-service conditions mean that tolerances will inevitably be less well controlled than in aerospace applications, and certainly very much worse than in the majority of past tests, this state of affairs must be of particular concern. Unlike the applications in the aerospace it is not possible to proof-test full-scale prototypes of the many and varied conditions prevailing for marine structures. Even if and when non-linear theories are able to precisely reproduce the deterministic behaviour of a given test, it is as yet unclear how they will be effectively incorporated into the design process. How, for example, can they be used to generate patterns of general behaviour and to isolate which parameters most crucially influence buckling performance? And over the immense possible range of geometries, support and loading conditions, how can they be used to generate data on imperfection sensitivity even for elastic systems, quite apart from that where material yield provides a further important controlling influence? Against this background it is clear: why expensive and time consuming non-linear analysis will in the near future be unlikely to provide an effective design tool; why testing alone over a sufficiently wide range of geometric and material parameters is unlikely to provide a purely empirical alternative; and, how simple, but reliable procedures for predicting lower bounds would provide such an attractive alternative.

But *what are the alternatives, and is it possible for axial loading to develop lower bound theories based upon the lines outlined above?*

#### *Reassessment of classical critical behaviour*

To isolate all the important components of membrane energy that contribute to the stabilisation of an axially loaded cylinder, it is necessary to provide a slightly modified form of classical critical load analysis. This has been more fully described for specific shell forms in previous publications[1-3] so that here only the briefest outline is provided.

Consider the orthotropically stiffened cylinder shown in Fig. 1. For illustration suppose that the boundary conditions conform with the classical simple support, and that under an axial load the prebuckled, fundamental, state of equilibrium may be approximated by the membrane stress resultants  $(N_x^F, N_\theta^F) \equiv (-\alpha_x t \sigma, 0)$ , where  $\sigma$  is the magnitude of the uniform axial tensile stress. The corresponding membrane strain state

$$(E_x^F, E_\theta^F) = \left[ -\frac{\alpha_\theta(\alpha_x - \mu^2)\sigma}{(\alpha_x\alpha_\theta - \mu^2)E}, +\frac{\mu(\alpha_x - \mu^2)\sigma}{(\alpha_x\alpha_\theta - \mu^2)E} \right]$$

will clearly not entirely satisfy the boundary constraints of even the simple support. The parameters  $\alpha_x$  and  $\alpha_\theta$  are respectively the ratios of the orthotropic axial and circumferential shell rigidities to that of the cylinder skin[2, 3], so that

$$\alpha_x = 1 + (1 - \mu^2) \frac{d_{x,t}}{S_{x,t}}$$

$$\alpha_\theta = 1 + (1 - \mu^2) \frac{d_{\theta,t}}{S_{\theta,t}}$$

with the shell geometry shown in Fig. 1. The Poisson's ratio is denoted by  $\mu$  and the modulus of elasticity by  $E$ . Later numerical studies, reported in relation to the test

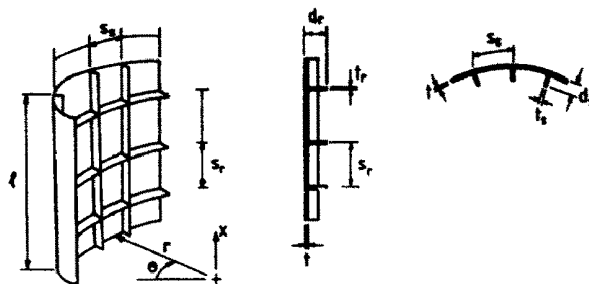


Fig. 1. Notation for geometry of orthotropically stiffened cylinder.

comparisons[15, 16], are based upon an exact solution for the fundamental states which required a non-linear, full bending, analysis of the prebuckled axisymmetric states, taking into account the empirically appropriate boundary conditions.

For an incremental displacement about this loaded and deformed fundamental state the incremental total potential energy,  $V$ , may be represented in the asymptotic form

$$V = V_0 + V_1 + V_2 + V_3 + \dots \tag{1}$$

where the notation  $V_i, i = 0, 1, 2, \dots$  is used to denote contributions that involve the  $i$ th power of the incremental displacements ( $u, v, w$ ). In this expansion the  $V_0$  term is of no present consequence,  $V_1$  is identically equal to zero (or strictly approximately zero if the membrane fundamental state is assumed), and it is the quadratic,  $V_2$ , term that in general provides the first non-zero contribution. It is of course this quadratic term that determines at what loads and in which modes the fundamental equilibrium states become critically stable; passing through such states are the secondary paths whose characteristics determine the type of post-buckling behaviour, which is governed by the nature of the higher order terms  $V_3, V_4, \dots$  in the expansion of eqn (1). For our present purposes, however, it is the  $V_2$  term that plays the crucial role.

Using conventional thin shell theory the quadratic term when expanded may be represented in the form

$$\begin{aligned} V_2 = & \frac{1}{2} \int [n'_x \epsilon'_x + n'_\theta \epsilon'_\theta + 2n'_{x\theta} \epsilon'_{x\theta}] r \, d\theta \, dx \\ & + \frac{1}{2} \int [m'_x \chi'_x + m'_\theta \chi'_\theta + 2m'_{x\theta} \chi'_{x\theta}] r \, d\theta \, dx \\ & + \frac{1}{2} \int [N_x^F \epsilon_x'' + n_x'' E_x^F] + [N_\theta^F \epsilon_\theta'' + n_\theta'' E_\theta^F] r \, d\theta \, dx \\ \equiv & U_M + U_B + \tilde{V}_M^x + \tilde{V}_M^\theta + \tilde{V}_M^{\theta} \end{aligned} \tag{2}$$

where  $(n_x, n_\theta, n_{x\theta})$  and  $(m_x, m_\theta, m_{x\theta})$  are the axial, hoop, shear or twist stress and moment resultants respectively, and  $(\epsilon_x, \epsilon_\theta, \epsilon_{x\theta})$  and  $(\chi_x, \chi_\theta, \chi_{x\theta})$  their corresponding strains. The single dash implies that the stress or strain is linearly related to the incremental displacements, while the double dash indicates that the appropriate stress or strain depends quadratically upon these displacements. The first and second integral represent what we could refer to as linear membrane,  $U_M$ , and bending,  $U_B$ , strain energy contributions, to reflect their origin in the linear strain-displacement relationships. The third integral is broken down into its four separate components which can be seen to result from the interaction between the fundamental state and the non-linear membrane actions associated with the incremental displacements.

Stabilisation of the shell against incremental displacements about the fundamental equilibrium states is provided by the linear strain energy  $U \equiv U_M + U_B$  and, most significantly for our present developments by the non-linear circumferential energy component

$$\tilde{V}_M^\theta = \frac{1}{2} \int n_\theta'' E_\theta^F r \, d\theta \, dx. \tag{3}$$

With the hoop strain  $E_{\theta}^F$  being axisymmetric it is only the axisymmetric bands of average non-linear hoop stress  $n_{\theta}''$  that provide a net contribution to  $\tilde{V}_M^{\theta}$ . The significance of this term so far as post-buckling behaviour is concerned will be discussed below. A conventional derivation of the critical loads in which all the terms  $\tilde{V}_M^x, \tilde{\tilde{V}}_M^x, \dots$  are lumped together to give

$$\tilde{V}_M^x + \tilde{\tilde{V}}_M^x + \tilde{V}_M^{\theta} + \tilde{\tilde{V}}_M^{\theta} \equiv -\alpha_x t \int \sigma \frac{1}{2} \left( \frac{\partial w}{\partial x} \right)^2 r \, d\theta \, dx$$

fails to identify the important stabilisation provided by the product of the fundamental hoop strain  $E_{\theta}^F$  and the non-linear hoop stress  $n_{\theta}''$  as represented by the term  $\tilde{\tilde{V}}_M^{\theta}$  in eqn (3). Of the other components arising from non-linear membrane action the term  $\tilde{V}_M^{\theta} \equiv 0$ , by virtue of  $N_{\theta}^F = 0$ , while the axial terms  $(\tilde{V}_M^x + \tilde{\tilde{V}}_M^x)$  provide the negative or destabilising contributions to the total potential energy. On the basis of this notation the classical critical stress,  $\sigma_c$ , may be represented as

$$\sigma_c = \frac{(U_M + U_B)}{(\tilde{V}_{M,\sigma}^x + \tilde{\tilde{V}}_{M,\sigma}^x + \tilde{\tilde{V}}_{M,\sigma}^{\theta})} \tag{4}$$

where

$$\tilde{V}_{M,\sigma}^x = \frac{d\tilde{V}_M^x}{d\sigma}$$

The implication of the above discussion is that in determining the critical stress  $\sigma_c$  associated with a critical mode having  $i$  waves in the circumferential direction and  $j$  half-waves in the axial direction, there is a certain stress  $\sigma_c^*$  above which the stability of the shell is entirely dependent upon the contribution coming from  $\tilde{\tilde{V}}_M^{\theta}$ . This is depicted in Fig. 2 which shows that below the stress level  $\sigma_c^*$  the system would be stable, that is  $V_2$  would be positive, even if the non-linear hoop energy  $\tilde{\tilde{V}}_M^{\theta}$  was not present. Between the stress level  $\sigma_c^*$  and the classical critical stress  $\sigma_c$  the system would be unstable if it were not for the stabilisation provided by  $\tilde{\tilde{V}}_M^{\theta}$ . Stress  $\sigma_c$  represents the classical critical stress at which  $V_2 = 0$ , and above which  $V_2 < 0$  and the fundamental equilibrium states would be unstable. The practical importance of the term  $\tilde{\tilde{V}}_M^{\theta}$  in stabilising the shell between  $\sigma_c^*$  and  $\sigma_c$  will be discussed in the next section. For present purposes we could simply observe that for a typical isotropic shell, as shown in Fig. 3, the separation between  $\sigma_c$  and  $\sigma_c^*$  increases as the axial wavelength increases ( $j$  decreases).

*Post-buckling behaviour*

The physical notions of post-buckling were identified at an early stage of the development of axial load buckling theories. Donnell in his important contribution of 1934[17] clearly outlined how in the post-critical behaviour a continuing deformation into the critical mode would involve the development of alternating bands of non-linear hoop

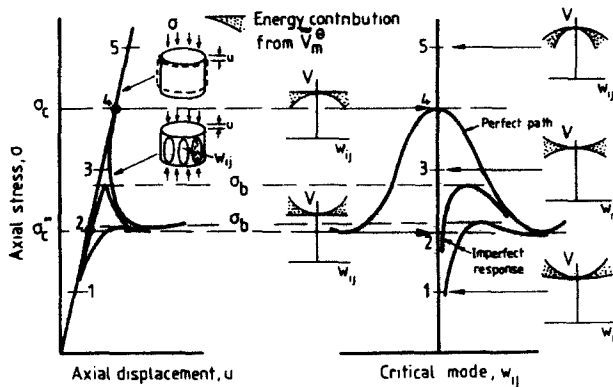


Fig. 2. Stability of paths.

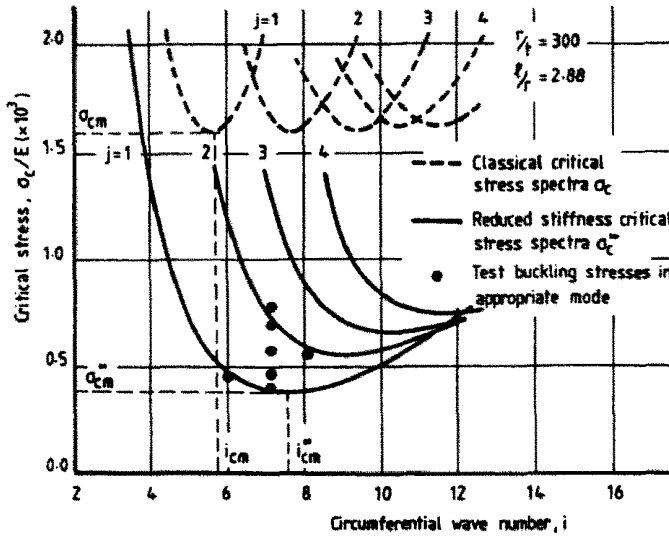


Fig. 3. Critical stress spectra for an isotropic cylinder.

stresses. These would represent the axisymmetric components of what we have here referred to as  $n_{\theta}^0$ . If it were not for an interaction with a certain axisymmetric deformation mode, having half the axial wavelength as the critical mode, these non-linear contributions, it was argued, would contribute to the continuing stabilisation of the shell. By identifying the nature of this coupling Donnell and many subsequent investigators have been able to ensure that the essential degrees of freedom have been retained in their attempted non-linear analysis of post-buckling.

These arguments are complementary to Koiter's reasoning, in his special theory[12], that a shell in an axisymmetric state with  $j$  axial half-waves will have a periodic distribution of circumferential tensile and compressive stresses. Buckling from this axisymmetric state into a non-axisymmetric mode would be induced in regions of compressive hoop stresses and hampered in regions of tensile hoop stresses, leading to the development of a non-axisymmetric buckling mode with nodal lines at the regions of maximum tensile hoop stresses, and therefore having twice the axial wavelength (or  $j/2$  axial half-waves) of the axisymmetric state.

What even Donnell's physically based notions did not make clear in his initial[17] and subsequent[18] discussions was why this coupling should actually lead to a loss of stiffness of the system. As originally stated, Donnell's arguments explained why a non-linear increase in stiffness, that would otherwise develop in the critical deformations of the shell, would not occur as a result of the propounded coupling action. If a loss of stiffness associated with an unstable post-buckling behaviour is to occur it is, of course, essential that the average non-linear hoop stresses  $n_{\theta}^0$  associated with this critical deformation, should have provided a positive contribution to the initial stiffness of the shell in its resistance to critical deformations. The above reanalysis of the critical behaviour provides this vital missing link. Now it becomes clear why Donnell's postulated post-critical coupling actually leads to a *loss* of stiffness of the shell.

As suggested in Fig. 2 deformations into a critical mode  $w_y$  would be accompanied by a rapid loss of the initial stiffness provided by the term  $\bar{V}_M^{\theta}$ . Even at exceedingly small critical deformations  $w_y$  it could be expected that the even smaller components of axisymmetric deformation needed to annihilate the initial stabilisation provided by the term  $\bar{V}_M^{\theta}$  would have developed. These axisymmetric coupling modes will therefore result in very little increase in energy, particularly for the long axial wavelengths in which  $\bar{V}_M^{\theta}$  produces its most significant stabilisation. Even without any other loss of membrane stiffness the axial load capacity would decrease until a plateau is reached at the load level  $\sigma_c^*$  for which  $V_2$  would just be critical even without the contribution from  $\bar{V}_M^{\theta}$ . Increasing imperfections in the form of the buckling mode  $w_y$  would for this unstable bifurcation have the effect of producing a rapid drop-off in the maximum buckling load capacity,  $\sigma_b$ , until for moderate levels of imperfections (of the order of the shell's thickness) the maximum

load would approach asymptotically the reduced stiffness critical load  $\sigma_c^*$ . It is these features that can be conveniently incorporated into a simplified analysis of the lower bounds to post-buckled loss of this stiffness.

#### Reduced stiffness lower bound buckling

If in the post-buckling behaviour a combination of the effects of the initial imperfections and mode coupling produces a situation where  $\tilde{V}_{M,\sigma}^0 \rightarrow 0$  then why not admit this and base a critical load analysis on the reduced total potential energy

$$V_2^* = U_M + U_B + \tilde{V}_{M,x}^x + \tilde{\tilde{V}}_{M,x}^x. \quad (5)$$

Exact analysis based upon this reduced energy (stiffness) model shows that the critical modes are almost identical with those predicted in the full energy classical analysis. As a consequence the so called reduced stiffness critical stress  $\sigma_c^*$ , based upon the expression

$$\sigma_c^* = \frac{(U_M + U_B)}{(\tilde{V}_{M,\sigma}^x + \tilde{\tilde{V}}_{M,\sigma}^x)} = \frac{(\tilde{V}_{M,\sigma}^x + \tilde{\tilde{V}}_{M,\sigma}^x + \tilde{\tilde{V}}_{M,\sigma}^0)}{(\tilde{V}_{M,\sigma}^x + \tilde{\tilde{V}}_{M,\sigma}^x)} \cdot \sigma_c \equiv \xi_{ij} \cdot \sigma_c \quad (6)$$

could be expected to provide reliable estimates of the exact values arising from stationarity of the reduced energy eqn (5).

With the terms  $\tilde{V}_{M,x}^x, \dots$  being almost entirely dependent upon the rotations about the tangents of the shell surface, the modal reduction factors,  $\xi_{ij}$  given as

$$\xi_{ij} \equiv \frac{(\tilde{V}_{M,\sigma}^x + \tilde{\tilde{V}}_{M,\sigma}^x + \tilde{\tilde{V}}_{M,\sigma}^0)}{(\tilde{V}_{M,\sigma}^x + \tilde{\tilde{V}}_{M,\sigma}^x)} \quad (7)$$

can be represented in particularly convenient forms. If for the general orthotropically stiffened cylinder of Fig. 1 it is assumed that the non-linear strains are with sufficient accuracy given by

$$\begin{aligned} \epsilon_x'' &= \frac{1}{2} \left( \frac{\partial w}{\partial x} \right)^2 \\ \epsilon_\theta'' &= \frac{1}{2} \left( \frac{\partial w}{r \partial \theta} \right)^2 \end{aligned} \quad (8)$$

then the various non-linear strain energy terms can be shown to take the form

$$\begin{aligned} \tilde{V}_{M,x}^x &= -\sigma \frac{K}{4} \int (\alpha_x - \mu^2) \left( \frac{\partial w}{\partial x} \right)^2 r \, d\theta \, dx \quad \equiv \sigma \tilde{V}_{M,\sigma}^x \\ \tilde{\tilde{V}}_{M,x}^x &= -\sigma \frac{K \alpha_\theta (\alpha_x - \mu^2)}{4(\alpha_x \alpha_\theta - \mu^2)} \int \left[ \alpha_x \left( \frac{\partial w}{\partial x} \right)^2 + \mu \left( \frac{\partial w}{r \partial \theta} \right)^2 \right] r \, d\theta \, dx \quad \equiv \sigma \tilde{\tilde{V}}_{M,\sigma}^x \\ \tilde{\tilde{V}}_{M,\sigma}^0 &= +\sigma \frac{K \mu (\alpha_x - \mu^2)}{4(\alpha_x \alpha_\theta - \mu^2)} \int \left[ \alpha_\theta \left( \frac{\partial w}{r \partial \theta} \right)^2 + \mu \left( \frac{\partial w}{\partial x} \right)^2 \right] r \, d\theta \, dx \quad \equiv \sigma \tilde{\tilde{V}}_{M,\sigma}^0 \end{aligned} \quad (9)$$

where  $K$  is the extensional rigidity of the shell wall.

Using these expressions and assuming that the critical displacements can be represented by the mode

$$w = w_{ij} \sin \frac{j\pi x}{l} \cos i\theta \quad (10)$$

the modal reduction factor may be expressed in the explicit form

$$\xi_{ij} = \frac{2(\alpha_x \alpha_\theta - \mu^2)}{(2\alpha_x \alpha_\theta - \mu^2) + \mu \alpha_\theta (i/\lambda)^2} \quad (11)$$



where  $\lambda = (j\pi)/(l/r)$ . The axial and circumferential wavelengths are  $l_x = 2l/j$  and  $l_\theta = 2\pi r/i$ , so that  $(i/\lambda) \equiv (l_x/l_\theta)$ . Assuming  $\mu^2 \ll 1$  eqn (11) can be approximated as

$$\xi_y \simeq \frac{1}{1 + \frac{1}{2} \left( \frac{\mu}{\alpha_x} \right) \left( \frac{i}{\lambda} \right)^2} \equiv \frac{1}{1 + \frac{1}{2} \left( \frac{\mu}{\alpha_x} \right) \left( \frac{l_x}{l_\theta} \right)^2} \tag{12}$$

which leads to the interesting observation that for orthotropically stiffened shells the potential reductions of buckling load in a given mode depend to large extent upon a single composite parameter

$$\mu_{eff} = \left( \frac{\mu}{\alpha_x} \right)$$

which could be regarded as an effective Poisson's ratio. This explicit form for the reduction factors leads to the important design analysis consideration that having once obtained the spectra of classical critical loads, and there are well established procedures for this, the reduced critical load spectra can be obtained directly from eqn (6) with the help of eqns (11) or (12). For boundary supports other than the simple supports the modal reduction factors can be obtained from the expression

$$\xi_y = \frac{1}{1 + \frac{1}{2} \left( \frac{\mu}{\alpha_x} \right) \left( \frac{i}{\lambda} \right)^2 k} \tag{13}$$

where the parameter  $k$  depends upon the degree of flexural restraint at the ends. For the simple support  $k = 1$ , while for a fully clamped support  $k = \frac{3}{4}$ .

The results of the reduced critical load analysis, based upon either the direct stationarity of eqn (5) or on the quotient of eqn (6), are shown for the previous example by the full lines in Fig. 3. What these reduced stiffness critical stress spectra show is that the potential reductions in buckling loads are greatest in the long axial wavelengths, and that there is a unique critical wavelength  $(i, j) = (i_{cm}^*, 1)$  for which the reduced stiffness critical stress takes on its minimum value,  $\sigma_{cm}^*$ . At this minimum reduced stiffness critical stress the potentially greatest knock-down in buckling load will occur. On this basis a theoretical knock-down factor.

$$\rho_{th} = \frac{\sigma_{cm}^*}{\sigma_{cm}} \tag{14}$$

can be defined, where  $\sigma_{cm}$  is the minimum critical stress of the shell obtained when using the full stiffness, or classical, method. This prediction of a unique mode for which the coupling described by Donnell will produce its potentially most severe reductions in buckling loads would appear to have considerable practical significance. But does it agree with the very considerable body of empirical evidence that is available for these shells?

BUCKLING TESTS ON AXIALLY LOADED CYLINDERS

The predictions from the reduced stiffness analysis represent at first sight a fairly radical departure from much of the conventional understanding of axial load buckling of cylinders. But a closer examination of past tests, and also some carefully conducted tests at University College London, suggest that in fact this simplified model provides a remarkably close representation of much previously inexplicable observed behaviour. The following comparisons are presented as being typical of the much wider studies of general elastic buckling of isotropic[19], and stringer[15] and ring[16] stiffened shells undertaken at University College London over the past few years. They are summarised here to show that there is in these experimental results a clearly established pattern of behaviour for which the reduced stiffness model provides an important unifying interpretive framework.

### Isotropic cylinders

The body of test data for this degenerate case of orthotropic stiffening is considerable. Perhaps the first feature of the reduced stiffness analysis that seems at odds with much of the literature is the prediction that, with moderate levels of random imperfections, buckling will be triggered by modes having long axial wavelengths and circumferential wavelengths that are determined by the geometry of the perfect cylinder rather than by the precise imperfection profile. But it is precisely this observation in the tests reported by Arbocz and Babcock[20] that has so far defied adequate theoretical explanation. These tests incorporated some of the most careful monitoring of the prebuckling growth of deformations ever undertaken. Figure 8(a) of Ref.[20] shows that in an isotropic shell having  $l/r = 2.0$ ,  $r/t = 862$  and  $\mu = 0.3$ , a clearly defined deformation has developed at a load 94% of the eventual buckling load. This triggering mode has a single half-wave in the axial direction and a circumferential distribution with dominant components from modes with circumferential wave numbers  $i = 9-11$ . Analysis of the same shell shows that the minimum reduced stiffness critical stress  $\sigma_{cm}^*/E = 0.10 \times 10^{-3}$  occurs with  $j = 1$  and  $i_{cm}^* = 10$ . The fact that the present lower bound appears to be a rather conservative estimate of the observed buckling stress  $\sigma_b/E = 0.47 \times 10^{-3}$  for this shell is a reflection of the very small initial imperfections (with a maximum component of the order of  $t/10$  in the buckling mode) present in these carefully manufactured test specimens. Even so, these same small imperfections were enough to bias the shell into a mode similar to that predicted by the reduced stiffness theory to provide the most likely potential buckling mode. Moreover, even though these imperfections were, predominantly composed of modes with a small number of circumferential waves,  $i = 0-3$ [20], the observed triggering mode agrees with the predicted reduced stiffness mode.

Where the imperfections become larger (of the order of the shell thickness) the reduced stiffness predictions provide increasingly reliable lower bound estimates of buckling loads in the long wavelength modes observed to trigger buckling. The shell having  $l/r = 2.88$ ,  $r/t = 300$  and  $\mu = 0.3$ , depicted in Fig. 3, was one of the geometries employed in Batista's recent test programme[21]. A number of tests on different specimens of nominally identical commercially available shells, having what appear to be practical levels of initial imperfection, have confirmed that despite considerable differences in initial imperfection profile the  $j = 1$  triggering mode having  $i_b$  between 7 and 8 agrees very closely with the lower bound prediction at  $i_{cm}^* = 8$ . The observed buckling stress,  $\sigma_b$ , ranged from 25 to 51% of the classical critical stress,  $\sigma_{cl}$ , compared with the predicted lower bound  $\sigma_{cm}^* = 0.24 \sigma_{cl}$ . These results are superimposed on the theoretical plots of Fig. 3.

Similar behaviour has been observed for other geometries[19-21], but unfortunately in the majority of test programmes data on the triggering modes, as opposed to the advanced post-buckled mode patterns, has not been obtained. In these cases it is necessary to rely upon information concerning the typically short axial wavelength diamond patterns associated with what are usually fairly advanced post-buckled states. However, in those cases where the triggering mode has been observed it appears that there is some correlation between the circumferential wavelengths of the short post-buckled modes and the long pre-buckled triggering modes. This has been commented upon and some qualitative comparisons have been included in ref.[20]. These observations appear to suggest that buckling into these short axial waves may occur as a result of the combination of the average axial stress together with the periodic components resulting from the growth of the long axial wavelength modes discussed above. A similar idea has recently been proposed for the prediction of lower bounds to elasto-plastic buckling loads[4].

As further evidence that the theoretical lower bounds from the reduced stiffness method provide practically realistic estimates of isotropic cylinder buckling consider the collected buckling data[19, 24] shown in Fig. 4. Although not generally recognised, when compiling the empirical data shown in Fig. 4, it was observed that the dependence of buckling stresses on  $l/r$  may extend well beyond the  $l/r = 0.5$  limit that is sometimes accepted[22]. This separate and at times considerable influence from  $l/r$  on buckling stresses is predicted by the reduced stiffness model[1]. Other factors that have been found by the reduced stiffness modelling to exert some controlling influence on the potential imperfection sensitivity are

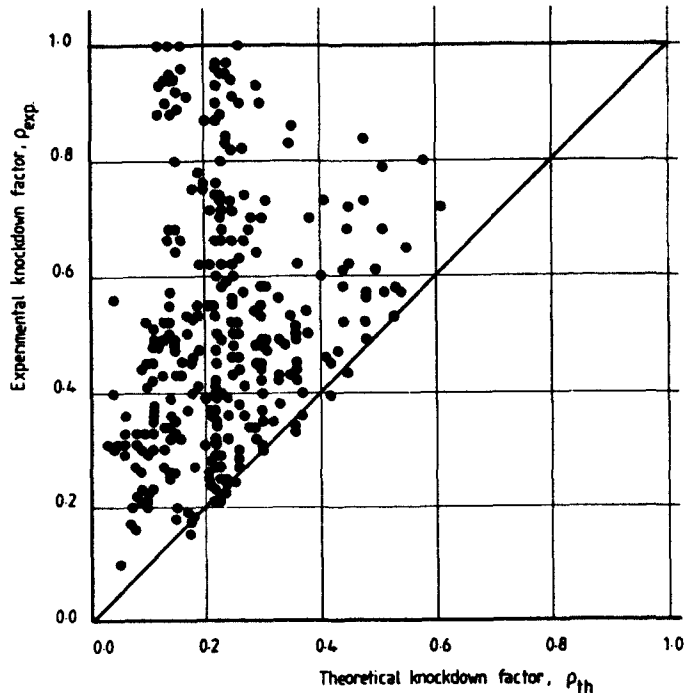


Fig. 4. Theoretical and experimental comparisons for isotropic cylinders.

the end boundary support conditions and the Poisson's ratio[1]. What Fig. 4 shows is that there is a fairly convincing correlation between the experimental data and the lower bound predictions of the present reduced stiffness method.

#### Stiffened cylinders

Orthotropically stiffened cylinders exhibit a classical bifurcation behaviour that has some differences to that for the isotropic cylinder. Perhaps most important is the consideration that the minimum classical critical load is generally associated with a uniquely defined critical mode; the isotropic cylinder as illustrated in Fig. 3 has the minimums associated with a wide range of axial wavelengths all occurring at the same load level. This is shown in Figs. 5 and 6 for examples of lightly stiffened stringer and ring stiffened cylinders respectively.

Provision of stringer stiffeners normally has the effect, shown in Fig. 5, of making the long axial wavelength  $j = 1$  modes dominant even in the classical critical analysis. Post-critical reductions due to the erosion of the still important  $\bar{V}_M^0$  terms have the effect of further reinforcing this likely importance of long axial wavelength modes. But as illustrated in Fig. 5 there is usually a slight shift in the circumferential wavelength  $i_{cm}^*$  at which the minimum reduced stiffness critical stress  $\sigma_{cm}^*$  occurs, compared with the wavelength  $i_{cm}$  associated with the minimum of the classical critical stress spectrum,  $\sigma_{cm}$ . The general buckling of most stringer stiffened shells takes this form with the degree of knock-down being dependent upon the precise form of the stiffening and shell geometry, as well as the boundary conditions.

For ring stiffened shells a classical analysis shows that the minimum of the critical stress spectrum is less well defined. The minimum, as illustrated in Fig. 6, is usually associated with a shortening of the axial wavelength, and often occurs in the axisymmetric mode for which  $i = 0$ . By considering a full non-linear analysis of the fundamental equilibrium path, which takes account of the appropriate end boundary conditions and the discreteness of the ring stiffeners[16], this axisymmetric buckling shows itself to be not a bifurcation but a non-linear "snap buckling" phenomenon. Taking into account the potential loss of stiffness in the post-buckling erosion of the term  $\bar{V}_M^0$ , the possible forms of buckling behaviour contrast strongly with those of the stringer stiffened shell. Maximum potential

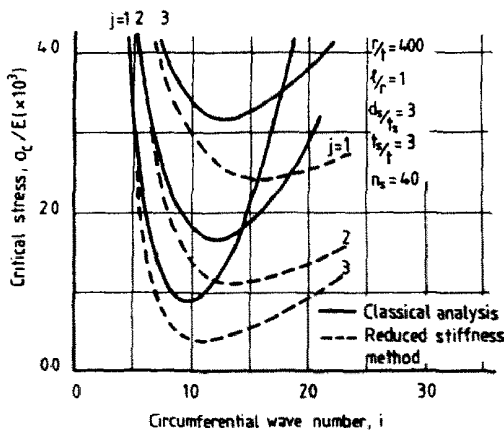


Fig. 5.

Fig. 5. Critical stress spectra for a stringer stiffened cylinder.

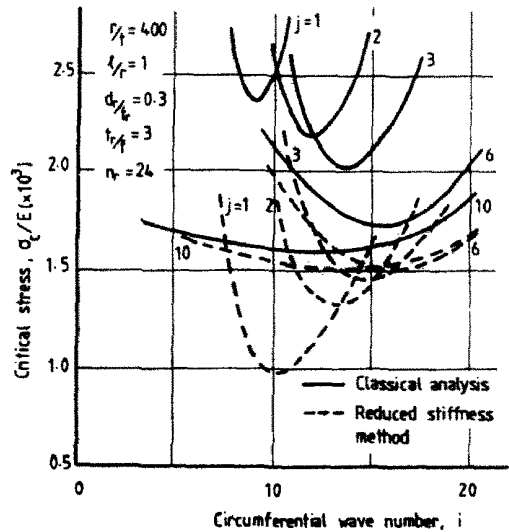


Fig. 6.

Fig. 6. Critical stress spectra for a ring stiffened cylinder.

loss of stiffness still occurs in the long axial wavelength modes for which  $j = 1$ . Whether these potential knock-downs of buckling load in the long axial wavelength modes are sufficient to bring  $\sigma_{cm}^*$  below the lowest of the short axial wavelength, axisymmetric, classical critical stresses,  $\sigma_{cm}$ , is dependent upon the precise form and extent of the ring stiffening. As a consequence, even for the general buckling of ring stiffened cylinders a transition in buckling behaviour is predicted to occur[3]. For lightly stiffened cylinders an imperfection sensitive buckling into a periodic mode of long axial wavelength would be expected. This form of buckling is closely related to that discussed above for the isotropic cylinder, whose behaviour can now be seen as simply part of the continuous and smooth changes of behaviour occurring as stiffening forms are modified. For heavily ring stiffened cylinders, in contrast, a relatively imperfection insensitive buckling into short axial wavelengths, usually having an axisymmetric form, is predicted to occur[3]. These two distinct forms of buckling have been observed in tests[23], and in the collected test data of Ref.[15] this test transition has been shown to conform with the predictions of the reduced stiffness model.

To affect reliable analysis of orthotropically stiffened cylinders, and consequently provide meaningful test comparisons, a number of analytical aspects need to be taken into account. Most of these considerations also apply to certain isotropic cylinders, but as a result of their stiffness or energy distributions in the classical critical behaviour, their importance would only be felt for shells having low values of  $l/r$  and  $r/t$ . The first important feature concerns the inclusion of geometric non-linearities in the fundamental axisymmetric behaviour. These arise as a result of the bending disturbances caused by the end boundary supports, and the eccentricity and discreteness of the stiffening. As demonstrated in Ref.[16] the replacement of the smeared orthotropic modelling by a discrete modelling of the ring stiffeners can have significant effects on the axisymmetric non-linear behaviour, which in turn exerts a strong influence on the spectrum of critical stresses for buckling into non-axisymmetric modes. Other factors that play an essential role in the following comparisons include: the proper treatment of end boundary constraints, including both static and kinematic eccentricity of the supports; the correct modelling of stiffener torsional stiffness; and the effects of eccentricity in the positioning of stiffeners[2, 3, 15, 16].

Recent detailed examination of all the elastic test results accessible to the authors, making use of the best available analysis techniques shows a remarkably close conformity

with the predictions of the reduced stiffness theory[15]. In Fig. 7 the summarised buckling loads for stringer stiffened cylinders are presented as experimental knockdown factors,  $\rho_{exp}$ , which represent the ratio of their buckling stresses to the corresponding minimum classical critical stresses. For each shell the theoretical knockdown factors,  $\rho_{th}$ , are defined in eqn (13) as the ratio of the minimum reduced stiffness critical stress to again the minimum classical critical stress. In presenting these results the test cylinders whose ends were fully clamped, usually in massive rings, have been plotted separately from those tested with simple support boundaries. In these latter tests considerable ambiguities surround the question of what the exact boundary stiffness would be at the instant of buckling. For this reason we have in our theoretical comparisons taken the most pessimistic estimate of the reductions in stiffness that may have conceivably taken place. It is possibly for this reason that some of the simple support results fall above the classical critical stress indicated by the line  $\rho_{exp} = 1$ . This, together with the consideration that many of these tests were carried out on carefully machined specimens for which the imperfections would conceivably be considerably less than those typical of full scale marine structures, makes it surprising that the present theoretical knockdowns provide as accurate lower bounds as those shown in Fig. 7. Particularly for the test specimens having the relatively more controlled clamped end supports, the considerable scatter of buckling loads is again convincingly bounded from below by the inclined line representing the reduced stiffness minimum critical loads  $\rho_{th}$ , and from above by the classical critical stress.

In comparing the test results for ring stiffened cylinders, the results have been separated according to whether they corresponded to lightly or heavily stiffened shells. In this context the division is equivalent to a separation as to whether buckling would be triggered by long axial wavelength modes for which  $\sigma_{cm}^* < \sigma_{cm}$ , or whether it would occur as an axisymmetric short axial wavelength mode for which  $\sigma_{cm}^* = \sigma_{cm}$ . The results are summarised in Fig. 8. The degree of scatter of buckling loads exhibited by the lightly ring stiffened cylinders, of Fig. 8(a) is again consistent with the upper and lower bounds predicted by classical and reduced stiffness theories. For the heavily stiffened shells where the classical and reduced stiffness critical loads would be identical, the scatter of test results about the perfect correlation line would appear to be consistent with the degree of accuracy in controlling

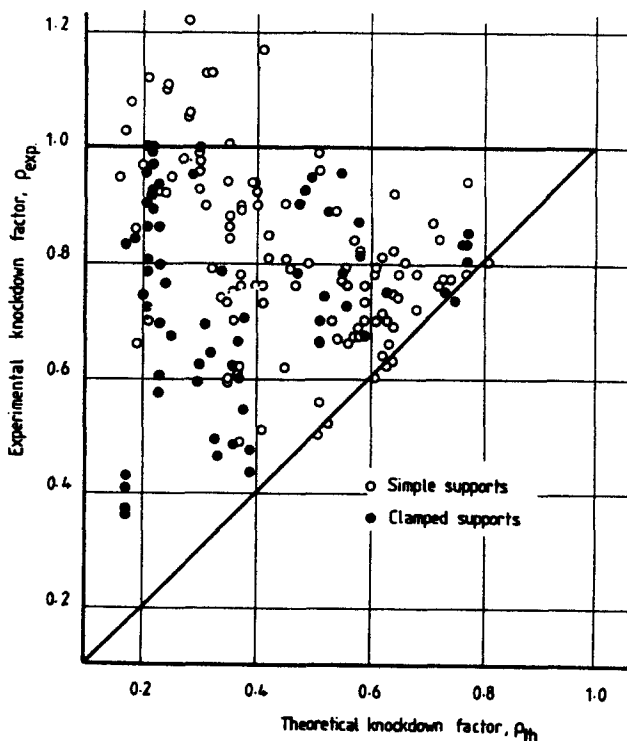


Fig. 7. Theoretical and experimental comparisons for stringer stiffened cylinders.

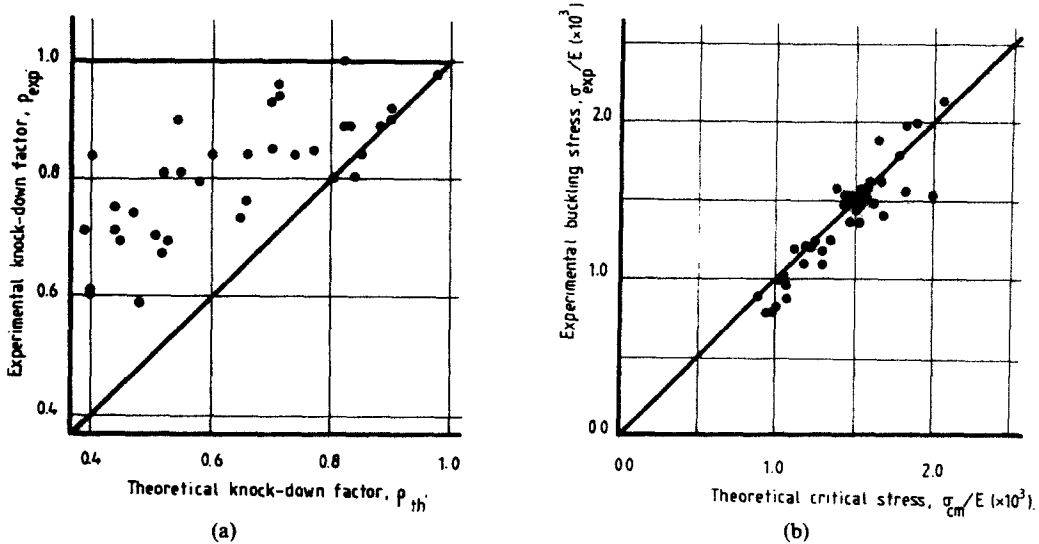


Fig. 8. Theoretical and experimental comparisons for (a) lightly, and (b) heavily ring stiffened cylinders.

the shell geometry, material properties and loading. Some of the reductions in buckling load, shown in Fig. 8(b), could also be associated with a loss of material stiffness accompanying the considerable geometric non-linearities producing the axisymmetric snap buckling for these test shells.

The importance of the above comparisons is that here for the first time is a theory capable of reproducing observed test behaviour over a wide range of shell and stiffener geometries. Isotropic cylinder buckling emerges as simply a special case of orthotropic cylinder buckling. The reduced stiffness model of post-critical loss of stiffness is found to closely predict the modes triggering buckling over the entire range of geometries. But perhaps more important for design, this simple theory provides lower bounds to the at times considerable scatter of test buckling loads.

#### DESIGN IMPLICATIONS

The reduced stiffness method has been shown to provide a unified description of the contrasting forms of general elastic buckling observed over a wide range of isotropic, ring and stringer stiffened axially loaded cylinders. This has allowed the unique status, that is sometimes ascribed to the isotropic cylinder, to be seen as merely a special case in the continuous change in buckling phenomena experienced over the broader class of orthotropic cylinder buckling. It has also enabled a number of previously unexplained experimental observations to be located within a single, physically explicit and analytically simple, framework. Indeed, the simplicity of the reduced stiffness method, the fact that it is based upon a straight-forward incorporation of physical descriptions of non-linear post-buckling behaviour, and the consideration that the method provides such agreeable confirmation of observed buckling modes and at the same time providing lower bounds to the scatter of their test buckling loads over almost the entire range of stiffened and unstiffened cylinder, commend the method as a potentially powerful design analysis tool. When extended to allow estimation of lower bounds for buckling that includes interaction between elastic and material non-linearities, as well as other combinations of loading, the method should provide a useful basis for the specification of design guidance notes.

But the general approach has other features which if exploited could be of considerable potential benefit in the process of conceptual design. Breaking down the cylinder's resistance to buckling into its component parts indicates to the designer which of the shell's stiffness components it would be most beneficial to modify if an improvement in elastic buckling is to be affected through the use of orthotropic stiffening. The following design study is typical of those that can be performed on the basis of the reduced stiffness method.

Consider a simply supported cylinder of fixed radius  $r = 4000$  mm, length  $l = 4000$  mm, and suppose that the total volume of steel has been fixed at  $1.55 \times 10^9$  mm<sup>3</sup>. For illustration assume that the number of equally spaced stringers is to be fixed at  $n_s = 40$  and that when rings are employed their number  $n_r = 24$ . The thickness of the stringers,  $t_s$ , and rings,  $t_r$ , will be taken to be fixed ratios of the cylinder skin thickness,  $t$ . Parameters  $\alpha_x$  and  $\alpha_\theta$  in this context provide a measure of the amount of material moved from the skin into the stringer and ring stiffeners respectively, and within the geometric constraints their specification automatically prescribes the aspect ratios  $d_s/t$ , and  $d_r/t$ , of the stiffeners, and consequently their bending stiffnesses.

Figure 9 shows that as material is moved from the skin into stringer stiffeners, that is  $\alpha_x$  increases while  $\alpha_\theta = 1.0$ , there is at first a reduction in the load carrying efficiency of the shell. The efficiency parameter,  $\eta$ , is a measure of the ratio of the minimum reduced stiffness critical load of the stiffened cylinder to that of the equivalent weight isotropic cylinder[2, 3]. The reason for this decline is that in the long axial wavelength periodic modes triggering buckling in this isotropic shell the circumferential bending is of considerable importance, while the axial bending energy provides a smaller contribution to the resistance to buckling[2]. Reducing the circumferential bending stiffness by decreasing the skin thickness has the effect of initially decreasing the total resistance to buckling deformations. Only when the increase in axial bending stiffness becomes considerable, and this occurs only at large  $\alpha_x$ , does this loss of circumferential bending energy (or stiffness) become compensated for by a concomitant increase in axial bending, and to a lesser extent membrane, energy. Eventually, the increases in axial bending energy are sufficient that they more than compensate the loss of the circumferential components. Eventually, an overall increase in resistance will occur. But it is evident in Fig. 9 that to achieve increase in elastic material efficiency through the use of stringers would require very heavy levels of stiffening in which  $\alpha_x$  is large, or very slender stiffeners having high  $d_s/t$ . This suggests that if in future design stringer stiffener topologies are to be adopted to improve elastic buckling strength, without introducing excessive fabrication problems, a trend towards increasing slender stiffener outstands might be expected. Such a tendency would need to be monitored very carefully to ensure that no interaction between general buckling and local stiffener tripping could take place.

Moving material from the skin into ring stiffeners has a sharply contrasting effect. The circumferential bending energy contribution, which is already large in the isotropic shell,

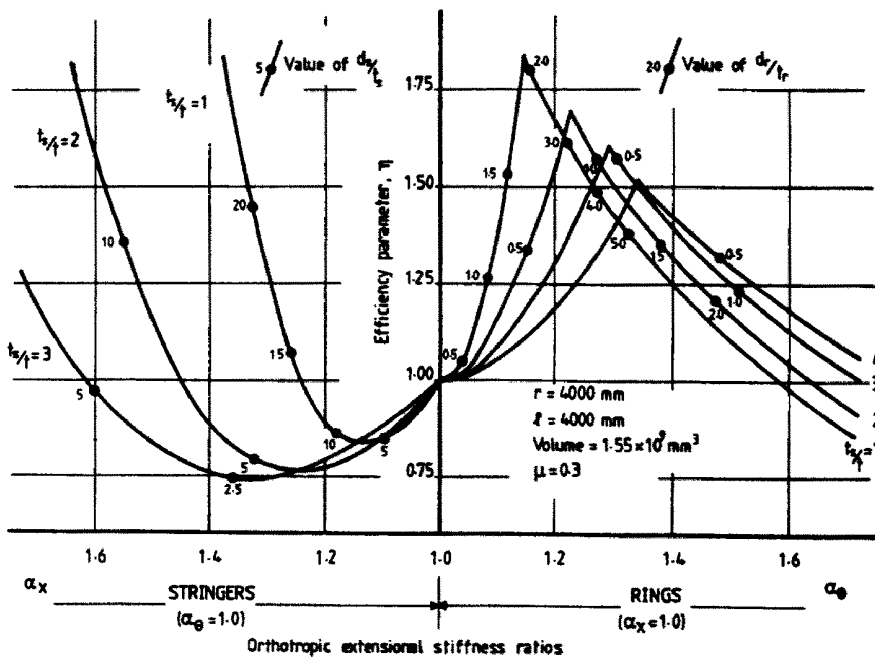


Fig. 9. Load carrying efficiency dependence on  $\alpha_x$  and  $\alpha_\theta$ .

is now rapidly increased. Since the axial bending energy contributes relatively little in the long axial wavelength triggering modes [3], its reduction through a loss of skin thickness is of little consequence. As a result the resistance to general buckling in these long axial wavelength modes is rapidly increased with even small quantities of ring stiffening, that is  $\alpha_\theta$  small. Eventually, a point is reached at which buckling into the long axial wavelength periodic modes occurs at loads greater than those associated with short axial wavelength modes. With the resistance to these short axial wavelength modes being dominated by axial bending energy [3], the use of decreasing skin thickness, associated with increasing  $\alpha_\theta$ , will result in a rapid drop-off in load carrying efficiency. It is for this reason that the lower bound carrying efficiency displays a strong optimum at the value of  $\alpha_\theta$  for which the long axial wavelength and short axial wavelength general modes have coincident buckling loads. The possible increases in load carrying capacity obtainable through the use of these optimum ring stiffening geometries appear to be considerable. This, combined with the evident fabrication advantages that could be exploited by use of the small squat ring stiffeners associated with these optimum designs, make these carefully dimensioned ring stiffeners an attractive practical proposition when elastic buckling is a major controlling influence on collapse.

### CONCLUSIONS

By identifying the components of the energy which provide a significant contribution in the initial resistance to buckling deformations, and which are lost in the imperfection sensitive mode couplings that occur in the post-buckling behaviour of axially loaded orthotropically stiffened cylinders, it has been possible to define an appropriate reduced stiffness buckling model. Analysis of this reduced stiffness model has a number of practically attractive features.

(1) In contrast with the classical analysis, it predicts the unique buckling modes observed to trigger the buckling of cylinders over a wide range of ring and stringer stiffener geometries. It shows how apparently unique forms of buckling experienced by isotropic cylinders can be viewed as simply special cases of the behaviour of orthotropically stiffened shells.

(2) Over a wide range of shell and stiffener geometries it provides lower bounds to the at times considerable scatter of test buckling loads.

(3) It achieves this on the basis of an analysis that has its origins in direct physical arguments, which in their turn help to clarify how and in what form the use of stiffeners is likely to improve the elastic buckling performance.

(4) By avoiding the complexities of non-linear analysis it allows for the possibility of encapsulating the lower bound predictions in simple forms that should be eminently suited to the requirements of design codes and guidance documents.

The general philosophy of the reduced stiffness method is advanced here as an illustration of the design advantages that accrue when the analyst is forced to consider what are the physical characteristics of behaviour. Its uniqueness and simplicity, and especially its lower boundedness, should recommend the method as a practical basis for the rational design of orthotropically stiffened cylinders.

*Acknowledgement*—The authors wish to acknowledge the support provided, for aspects of this work, by the Science Research Council of Great Britain made available through grants to the London Centre for Marine Structures and Materials.

### REFERENCES

1. J. G. A. Croll and R. C. Batista, Explicit lower bounds for the buckling of axially loaded cylinders. *Int. J. Mech. Sci.* **23**, 331–343 (1981).
2. C. P. Ellinas, R. C. Batista and J. G. A. Croll, Overall buckling of stringer stiffened cylinders. *Proc. Inst. Civ. Engrs*, Part 2, **71**, 479–512 (1981).
3. C. P. Ellinas and J. G. A. Croll, Overall buckling of ring stiffened cylinders. *Proc. Inst. Civ. Engrs*, Part 2, **71**, 637–661 (1981).
4. J. G. A. Croll, Lower bound-plastic buckling of cylinders. *Proc. Inst. Civ. Engrs*, Part 2, **71**, 235–261 (1981).
5. S. E. Svenson and J. G. A. Croll, Interaction between local and overall buckling. *Int. J. Mech. Sci.* **17**, 307–321 (1975).
6. J. G. A. Croll, Model of interactive buckling of stiffened plates. *J. Engng Mech. Div., ASCE* **101**, EM5, 575–591 (1975).



7. J. M. T. Thompson, *et al.*, An experimental study of imperfection sensitivity in the buckling of stiffened plates. In *Buckling of Structures, Proc. IUTAM Symp., Harvard, Cambridge, U.S.A., June 1974*, p. 149. Springer-Verlag, Berlin (1976).
8. C. P. Ellinas and J. G. A. Croll, Post-critical analysis of torsionally buckled stiffener plates. *Int. J. Solids Structures* 17, 11–27 (1981).
9. R. C. Batista and J. G. A. Croll, A design approach for unstiffened cylindrical shells under external pressure. *Proc. Int. Conf. on Thin-walled Structures*, University of Strathclyde, April 3–6, 1979.
10. J. Arbocz, Past, present and future of shell stability analysis. Delft University of Technology, Department of Aerospace Engng, Rep. LR-320, 1981.
11. R. C. Tennyson and D. B. Muggeridge, Buckling of axisymmetric imperfect circular cylindrical shells under axial compression. *AIAA J.* 7, 2127–2131 (1969).
12. W. T. Koiter, The effect of axisymmetric imperfections on the buckling of cylindrical shells under axial compression. *Proc. Kon. Ned. Ak. Wet.* B66, 265 (1963).
13. N. Yamaki, Post-buckling and imperfection sensitivity of circular cylindrical shells under compression. In *Theoretical and Applied Mechanics* (Edited by W. T. Koiter) North-Holland, Amsterdam (1976).
14. M. Esslinger and B. Geier, *Postbuckling behaviour of structures*. Springer-Verlag, Wein (1975).
15. C. P. Ellinas and J. G. A. Croll, *Experimental and Theoretical Correlations for Axially Compressed Stringer Stiffened Shells*. London Centre for Marine Technology, London (1981); *J. Strain Analysis* 18(1) (1983).
16. C. P. Ellinas and J. G. A. Croll, *Experimental and Theoretical Correlations for Axially Compressed Ring Stiffened Shells*. London Centre for Marine Technology, London (1981); *J. Strain Analysis* 18(2) (1983).
17. L. H. Donnell, A new theory for the buckling of thin cylinders under axial compression and bending. *Trans. ASME* 56, 795 (1934).
18. L. H. Donnell and C. C. Wan, Effect of imperfections on buckling of thin cylinders and columns under axial compression. *J. Appl. Mech.* 17, 73–83 (1950).
19. R. C. Batista and J. G. A. Croll, A design approach for axially compressed unstiffened cylinders. In *Stability Problems in Engineering Structures and Components* (Edited by T. H. Richards and P. Stanley). Applied Science, London (1979).
20. J. Arbocz and C. D. Babcock, The effect of general imperfections on the buckling of cylindrical shells. *J. Appl. Mech.* 36, 28–38 (1969).
21. R. C. Batista, Lower bound estimates for cylindrical shell buckling. Ph.D. Dissertation, University of London, 1979.
22. V. I. Weingarten *et al.*, Elastic stability of thin-walled cylindrical and conical shells under axial compression. *AIAA J.* 3, 500–505 (1965).
23. J. Singer, J. Arbocz and C. D. Babcock, Buckling of imperfect stiffened cylindrical shells under axial compression. *AIAA, J.* 9, 68–75 (1971).
24. C. P. Ellinas and J. G. A. Croll, *Experimental and Theoretical Correlations for Axially Compressed Isotropic Cylinders*. London Centre for Marine Technology, London (1983).